Chapter 2
LEAP-ASIA-2019 Simulation Exercise: Calibration of Constitutive Models and Simulations of the Element Tests

Kyohei Ueda, Yoshikazu Tanaka, Anurag Sahare, Ahmed Elgamal, Zhijian Qiu, Rui Wang, Tong Zhu, Chuang Zhou, Jian-Min Zhang, Andres Reyes Parra, Andres Barrero, Mahdi Taiebat, Waka Yuyama, Susumu Iai, Junichi Hyodo, Koji Ichii, Mohamed A. Elbadawy, Yan-Guo Zhou, Gianluca Fasano, Anna Chiaradonna, Emilio Bilotta, Pedro Arduino, Mourad Zeghal, Majid Manzari, and Tetsuo Tobita

Abstract This chapter presents a summary of the calibration exercises (i.e., element test simulations) submitted by nine numerical simulation teams that participated in the LEAP-ASIA-2019 prediction campaign. The standard sand selected for the campaign is Ottawa F-65, and researchers have developed several efforts to increase the database of laboratory tests to characterize the physical and mechanical properties of this sand (Carey TJ, Stone N, Kutter BL, Grain Size Analysis and Maximum and Minimum Dry Density of Ottawa F-65 Sand for LEAP-UCD-2017. Model tests and numerical simulations of liquefaction and lateral spreading: LEAP-UCD-2017. Springer, 2019; El Ghoraiby MA, Park H, Manzari MT. Physical and mechanical properties of Ottawa F65 sand. In: Model tests and numerical simulations of liquefaction and lateral spreading: LEAP-UCD-2017, Springer, 2019; Ueda K, Vargas RR, Uemura K, LEAP-Asia-2018: Stress-strain response of Ottawa sand in Cyclic Torsional Shear Tests, DesignSafe-CI [publisher], Dataset, https://doi.org/10.17603/DS2D40H, 2018; Vargas RR, Ueda K, Uemura K, Soil Dyn Earthq

K. Ueda (✉) · Y. Tanaka · A. Sahare
Disaster Prevention Research Institute, Kyoto University, Kyoto, Japan
e-mail: ueda.kyohei.2v@kyoto-u.ac.jp

A. Elgamal · Z. Qiu
Department of Structural Engineering, University of California San Diego, La Jolla, CA, USA

R. Wang · T. Zhu · C. Zhou · J.-M. Zhang
Department of Hydraulic Engineering, Tsinghua University, Beijing, China

A. R. Parra · A. Barrero · M. Taiebat
Department of Civil Engineering, University of British Columbia, Vancouver, BC, Canada

W. Yuyama · S. Iai
FLIP Consortium, Kyoto, Japan

T. Tobita et al. (eds.), *Model Tests and Numerical Simulations of Liquefaction and Lateral Spreading II*, https://doi.org/10.1007/978-3-031-48821-4_2

Eng 133:106111, 2020; Vargas RR, Ueda K, Uemura K, Dynamic torsional shear tests of Ottawa F-65 Sand for LEAP-ASIA-2019. Model tests and numerical simulations of liquefaction and lateral spreading: LEAP-ASIA-2019, Springer, 2023). The objective of this element test simulation exercise is to assess the performance of the constitutive models used by the simulation teams for simulating the experimental results of a series of undrained stress-controlled cyclic torsional shear tests on Ottawa F-65 sand for two different relative densities (Dr = 50% and 60%) (Ueda K, Vargas RR, Uemura K, LEAP-Asia-2018: Stress-strain response of Ottawa sand in Cyclic Torsional Shear Tests, DesignSafe-CI [publisher], Dataset, https://doi.org/10.17603/DS2D40H, 2018; Vargas RR, Ueda K, Uemura K, Soil Dyn Earthq Eng 133:106111, 2020; Vargas RR, Ueda K, Uemura K, Dynamic torsional shear tests of Ottawa F-65 sand for LEAP-ASIA-2019. Model tests and numerical simulations of liquefaction and lateral spreading: LEAP-ASIA-2019, Springer, 2023). The simulated liquefaction strength curves demonstrate that majority of the constitutive models are capable of reasonably capturing the measured liquefaction strength curves both for Dr = 50% and 60%. However, the simulated stress paths and stress-strain relationships show some differences from the corresponding laboratory tests in some cases.

J. Hyodo
Tokyo Electric Power Services, Tokyo, Japan

K. Ichii
Faculty of Societal Safety Science, Kansai University, Osaka, Japan

M. A. Elbadawy · Y.-G. Zhou
Department of Civil Engineering, Zhejiang University, Hangzhou, People's Republic of China

G. Fasano · A. Chiaradonna · E. Bilotta
Department of Civil, Architectural and Environmental Engineering, University of Naples Federico II, Naples, Italy

P. Arduino
Department of Civil and Environmental Engineering, University of Washington, Seattle, WA, USA

M. Zeghal
Department of Civil and Environmental Engineering, Rensselaer Polytechnic Institute, Troy, NY, USA

M. Manzari
Department of Civil and Environmental Engineering, George Washington University, Washington, DC, USA

T. Tobita
Department of Civil, Environmental and Applied Systems Engineering, Kansai University, Osaka, Japan

Keywords Liquefaction Experiments and Analysis Projects (LEAP-ASIA-2019) · Numerical simulation · Constitutive model · Ottawa F-65 · Liquefaction strength curve

2.1 Introduction

The LEAP-ASIA-2019 project involved nine numerical simulation teams from different academic institutions and geotechnical companies from around the world; they participated in the modeling of some of the centrifuge model experiments performed at several research institutions. The simulation exercise consisted of the calibration of constitutive model parameters, Type-B predictions, and Type-C predictions. This chapter presents an overview of the results of the first phase (i.e., model calibration) of this exercise. The main objective of this phase was to provide the numerical simulation teams with the opportunity to calibrate their constitutive models, which will be used in the Type-B simulations, using the results of cyclic shear tests performed on Ottawa F-65 sand during the LEAP-2019 project.

For the calibration phase of constitutive models, a series of hollow cylinder torsional shear tests were performed at Kyoto University (KyU) for Ottawa F-65 sand with a relative density (Dr) of 50% and 60% under an initial effective confining stress of 100 kPa. Also, direct simple shear tests were performed at George Washington University (GWU) for Dr = 71% under an initial effective vertical stress of 100 kPa and Dr = 69% under 40 kPa.

The element tests mentioned above provided new datasets that complement the monotonic and cyclic triaxial shear tests reported by Vasko (2015) and Vasko et al. (2018), monotonic and cyclic simple shear tests by Bastidas (2016) and Bastidas et al. (2017), and cyclic triaxial tests by El Ghoraiby and Manzari (2018) and El Ghoraiby et al. (2019). These tests were previously made available to the numerical simulation teams that participated in the numerical simulation of the LEAP-2017 project. The new datasets were made available to all the numerical simulation teams that participated in the LEAP-2019 project via DesignSafe, as described below.

The timeline for this calibration phase of the LEAP-2019 project was as follows:

1. All the element test data were made available on DesignSafe to the numerical simulation teams by December 5, 2018. These are as follows:
    - LEAP-2015 GWU Laboratory Tests: https://doi.org/10.17603/DS2TH7Q
    - LEAP-2017 GWU Laboratory Tests: https://doi.org/10.17603/DS2210X (cyclic triaxial shear tests for Dr = 71%, 87%, and 97% at GWU).
    - LEAP-2018 GWU Cyclic Simple Shear: https://doi.org/10.17603/DS2HX3H (cyclic direct simple shear tests for Dr = 71% and 69% at GWU).
    - LEAP-2018 KyU Cyclic Torsional Shear: https://doi.org/10.17603/DS2D40H (cyclic torsional shear tests for Dr = 50% and 60% at KyU).

2. The participating teams were requested to simulate a selected number of the provided test data and liquefaction strength curves that were obtained from cyclic direct simple shear tests and cyclic torsional shear tests. The critical tests to be simulated were the cyclic torsional shear test for Dr = 50% and 60% (under an initial effective confining stress of 100 kPa). It was required to compare the simulated stress paths and stress-strain responses to the experimental results reported by KyU. If time allowed, it was desirable to show the validity of constitutive models for the other experimental results having higher relative densities. The numerical simulation team submitted the results of their element test simulations and comparisons with those of the provided element tests in the form of a detailed report by January 11, 2019.

2.2 The Numerical Simulation Teams

Table 2.1 shows the numerical simulation teams who submitted their calibration reports and participated in the Type-B simulation exercise. The constitutive model and the analysis platform used by each numerical simulation team are also listed in the table. Mode-detailed information of each constitutive model and the numerical simulation techniques used by each simulation team are provided in separate papers (Tanaka et al., 2023; Hyodo & Ichii, 2023; Fasano et al., 2023; Qiu & Elgamal, 2023; Elbadawy & Zhou, 2023; Reyes et al., 2023; Wang et al., 2023).

2.3 Results of the Element Test Simulations

Figures 2.1, 2.2, 2.3 and 2.4 show a detailed comparison of the numerical simulations of the undrained cyclic torsional shear tests on Ottawa F-65 sand for Dr = 50% with different cyclic stress ratios (i.e., CSR = 0.19, 0.15, 0.13, and 0.10). The

Table 2.1 Numerical simulation teams

No.	Numerical simulation team	Constitutive model	Analysis platform
1	Kyoto university (two different predictors)	Cocktail glass model	FLIP ROSE
2			
3	FLIP consortium	Cocktail glass model	FLIP ROSE
4	Tokyo electric power services	Cocktail glass model	FLIP ROSE
5	University of Naples Federico II	PM4Sand model	PLAXIS
6	University of Washington	PM4Sand model	OpenSees
7	University of California, san Diego	PDMY02 model	OpenSees
8	Zhejiang university	PDMY02 model	OpenSees
9		CPSP model	
10	University of British Columbia	SANISAND model	FLAC3D
11	Tsinghua University	CycLiqCP model	OpenSees

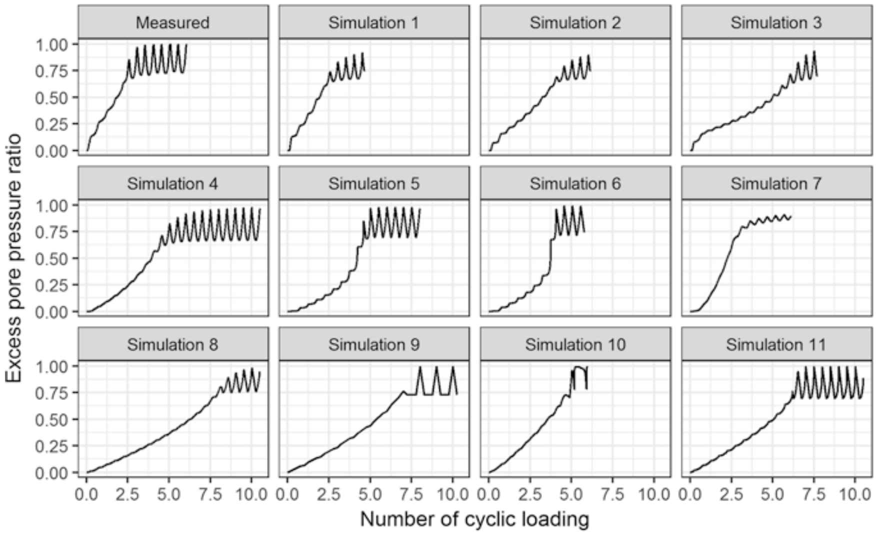

(a)

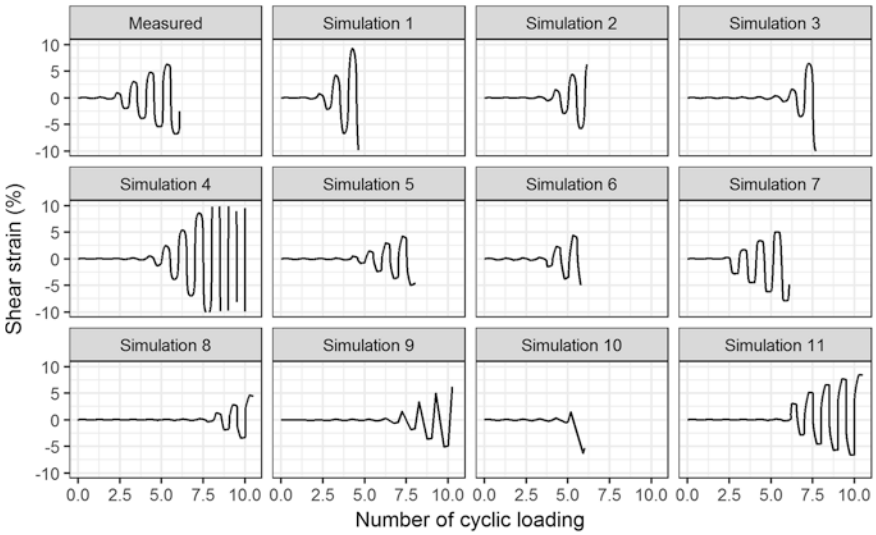

(b)

Fig. 2.1 Comparison of the numerical simulations of an undrained cyclic torsional shear test on Ottawa F-65 sand for Dr = 50%, CSR = 0.19. (**a**) Time history of excess pore pressure ratio, (**b**) Time history of shear strain, (**c**) Effective stress path, (**d**) Shear stress-shear strain relationship

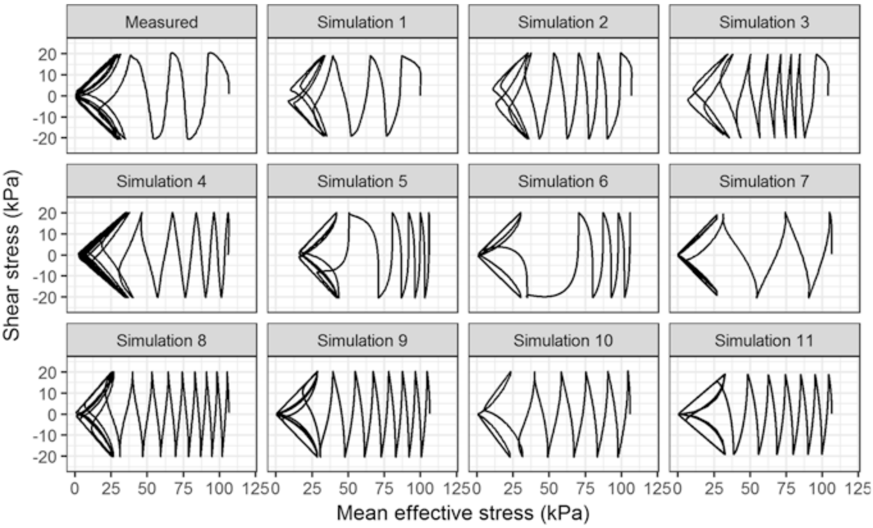

(c)

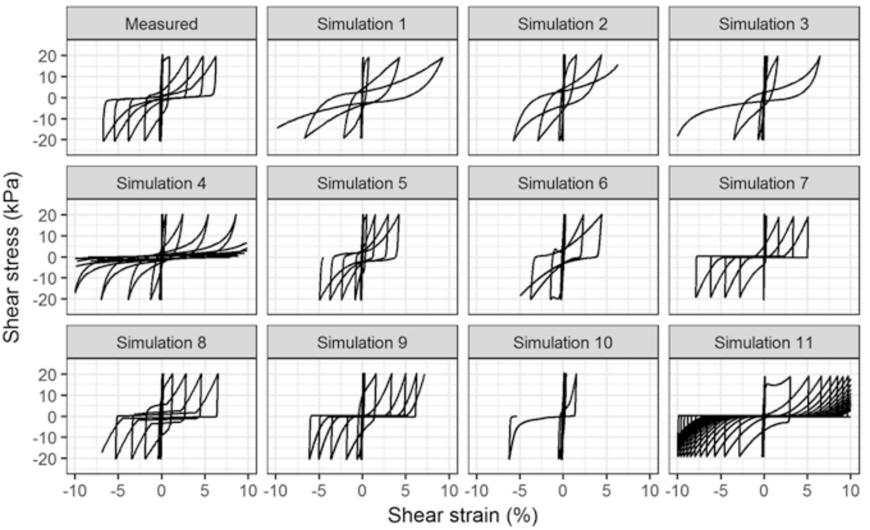

(d)

Fig. 2.1 (continued)

simulations are labeled Simulations 1 to 11. The numbers refer to the order of the simulation teams in the table presented above. The numerical simulation teams 1 and 2 belonging to the same organization used the same analysis platform with the same constitutive model, but they are distinguished because they carried out the

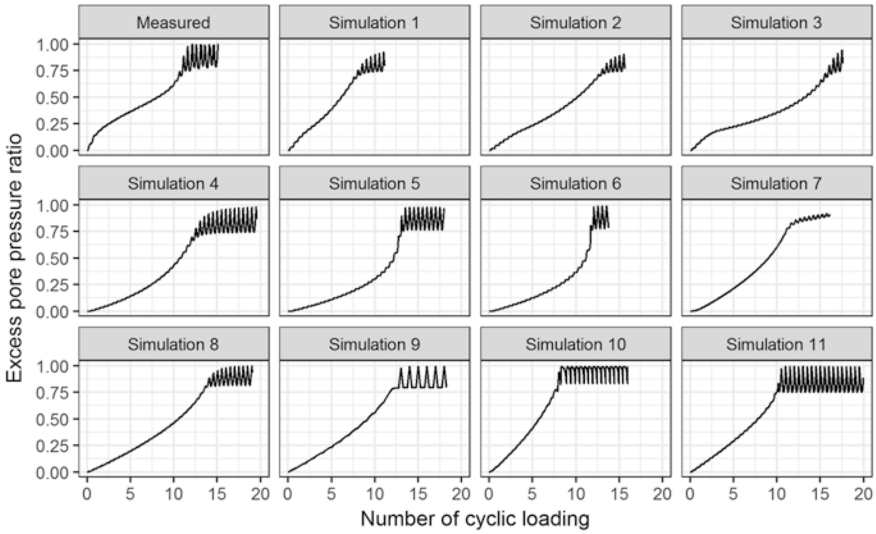

(a)

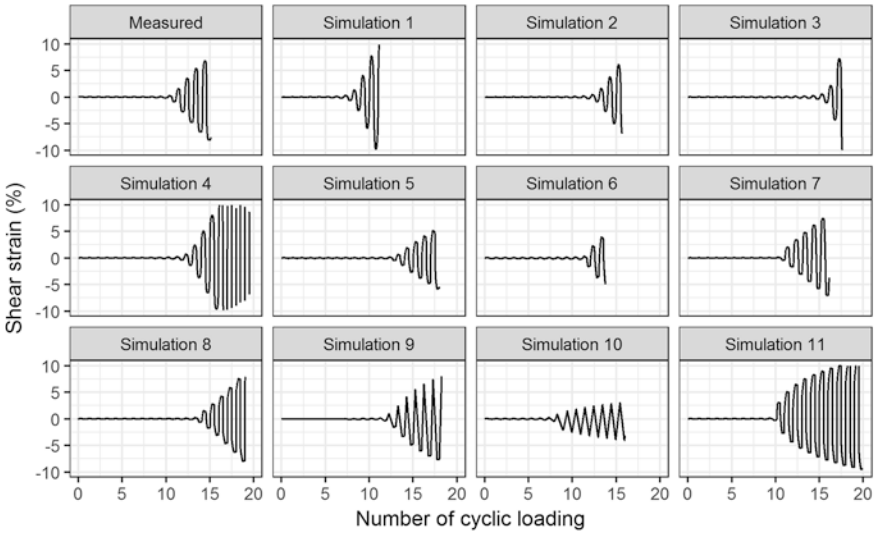

(b)

Fig. 2.2 Comparison of the numerical simulations of an undrained cyclic torsional shear test on Ottawa F-65 sand for Dr = 50%, CSR = 0.15. (**a**) Time history of excess pore pressure ratio, (**b**) Time history of shear strain, (**c**) Effective stress path, (**d**) Shear stress-shear strain relationship

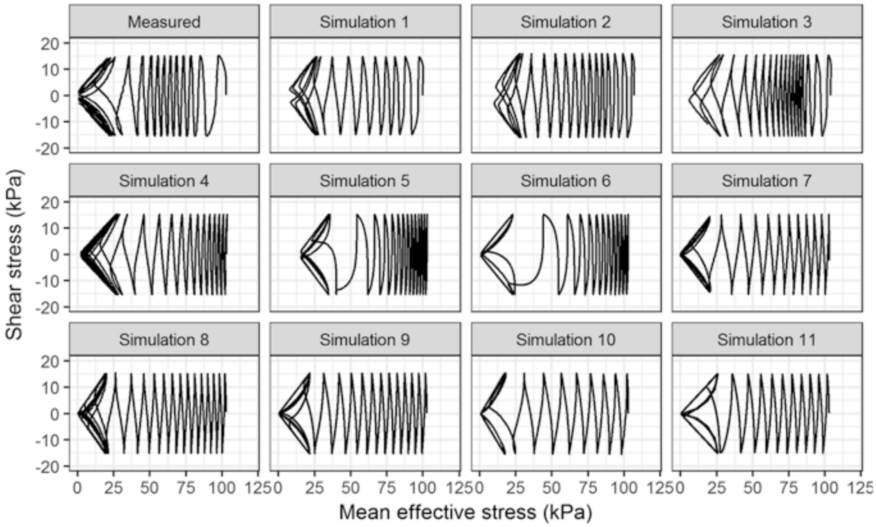

(c)

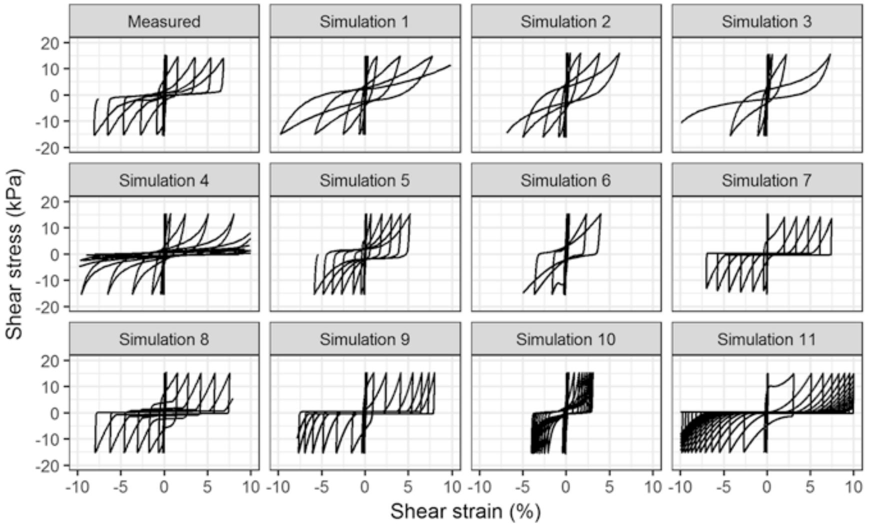

(d)

Fig. 2.2 (continued)

calibration independently. It is also noted that the same predictor performed Simulations 8 and 9, but they are distinguished because different constitutive models were used in the simulations. Figures 2.5, 2.6, 2.7, 2.8 and 2.9 show a similar comparison of the numerical simulations of the undrained cyclic torsional shear tests for Dr = 60% with different cyclic stress ratios (i.e., CSR = 0.20, 0.18, 0.15, 0.13, and 0.12). The numerical simulation team 3 did not submit simulations for Dr = 60% with CSR of 0.12.

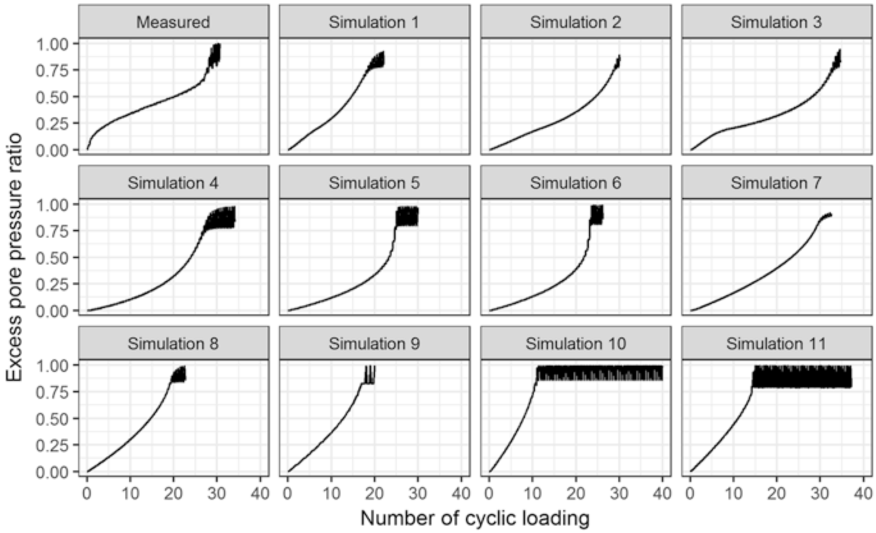

(a)

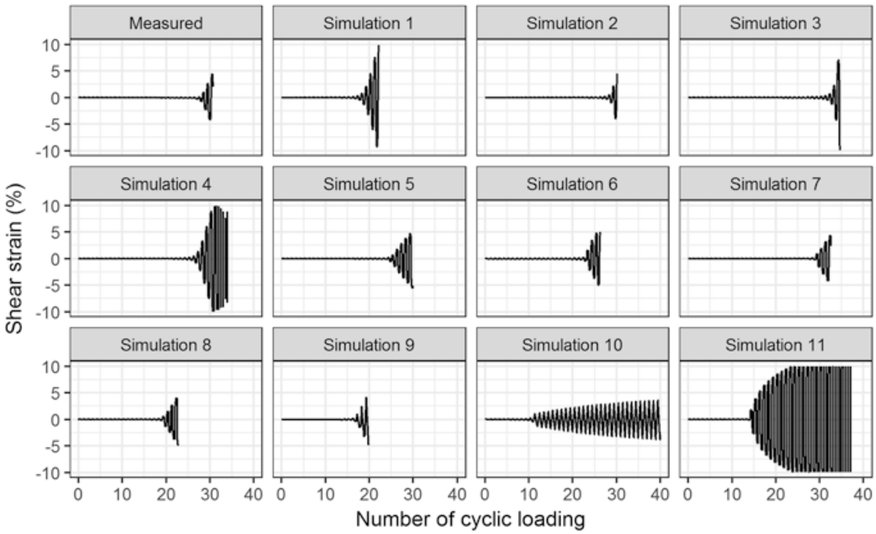

(b)

Fig. 2.3 Comparison of the numerical simulations of an undrained cyclic torsional shear test on Ottawa F-65 sand for Dr = 50%, CSR = 0.13. (**a**) Time history of excess pore pressure ratio, (**b**) Time history of shear strain, (**c**) Effective stress path, (**d**) Shear stress-shear strain relationship

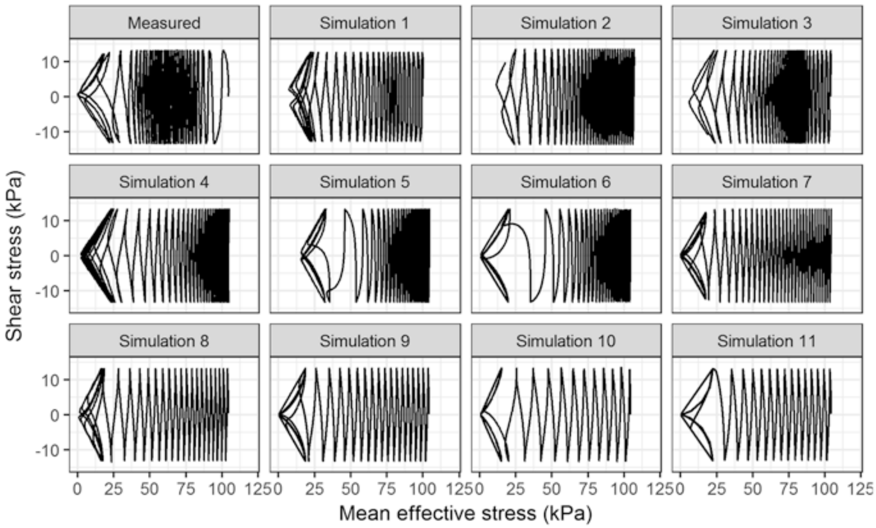

(c)

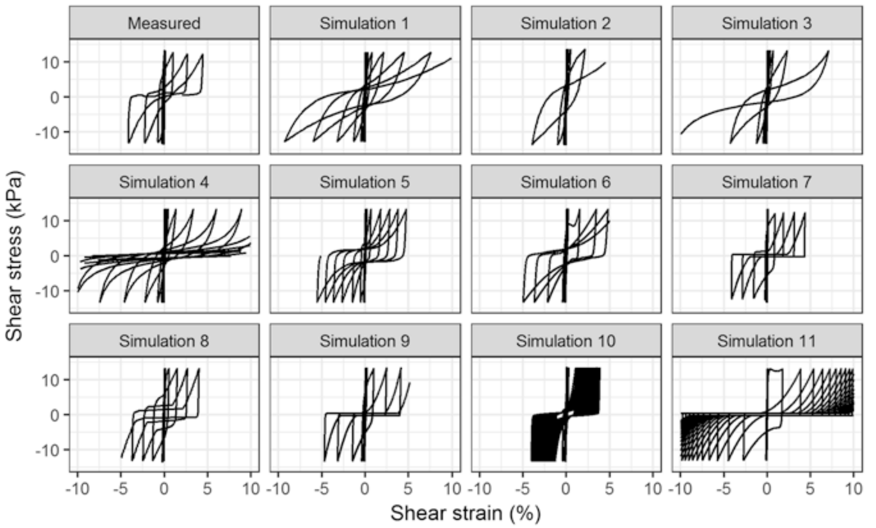

(d)

Fig. 2.3 (continued)

A review of Figs. 2.1, 2.2, 2.3, 2.4, 2.5, 2.6, 2.7, 2.8 and 2.9 indicates the following trends:

1. The majority of the constitutive models are capable of reasonably capturing the overall trends of the measured time histories of excess pore pressure ratio and shear strain, effective stress paths, and stress-strain responses both for Dr = 50% and 60%.

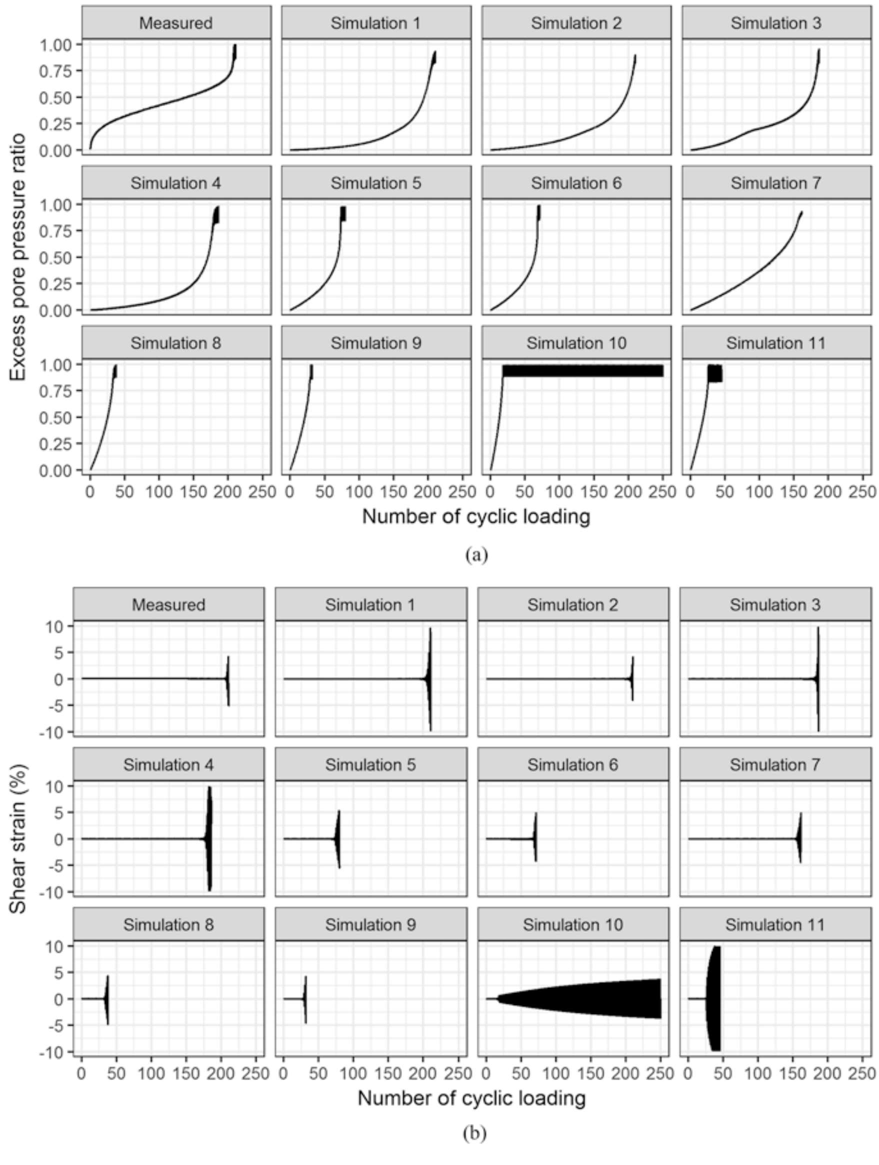

Fig. 2.4 Comparison of the numerical simulations of an undrained cyclic torsional shear test on Ottawa F-65 sand for Dr = 50%, CSR = 0.10. (**a**) Time history of excess pore pressure ratio, (**b**) Time history of shear strain, (**c**) Effective stress path, (**d**) Shear stress-shear strain relationship

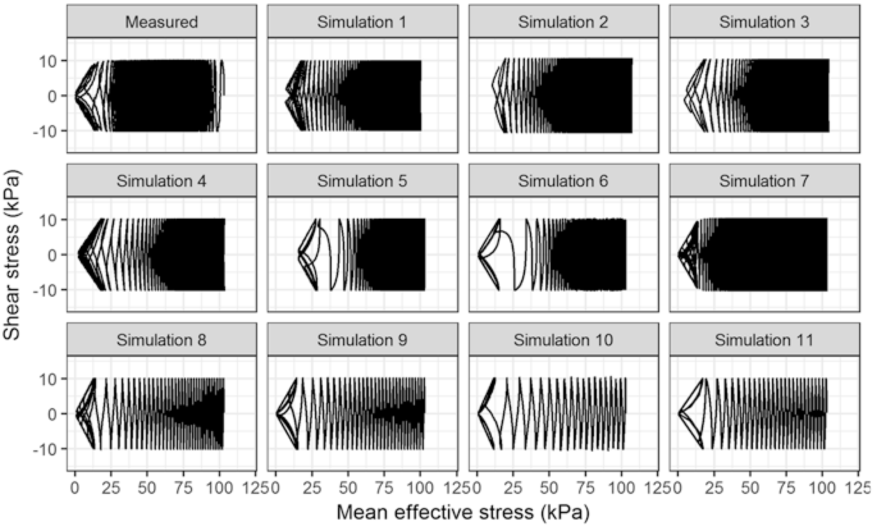

(c)

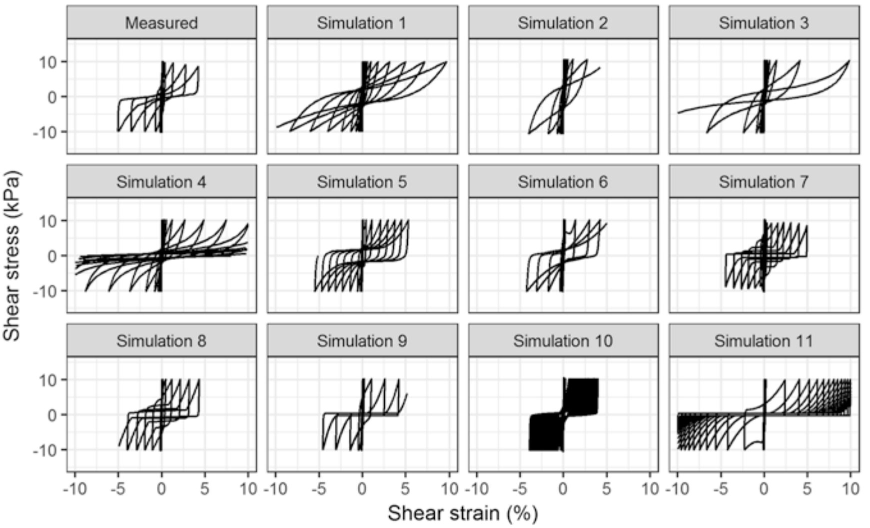

(d)

Fig. 2.4 (continued)

2. Simulations 1–4: Since the constitutive model and the analysis platform are the same, the simulated results are similar to some extent. However, different responses are observed depending on the model parameters; there are many cases where the effective stress path does not reach the origin (i.e., complete liquefaction) in Simulations 1 and 2, but it almost reaches the origin in Simulations 3 and 4.

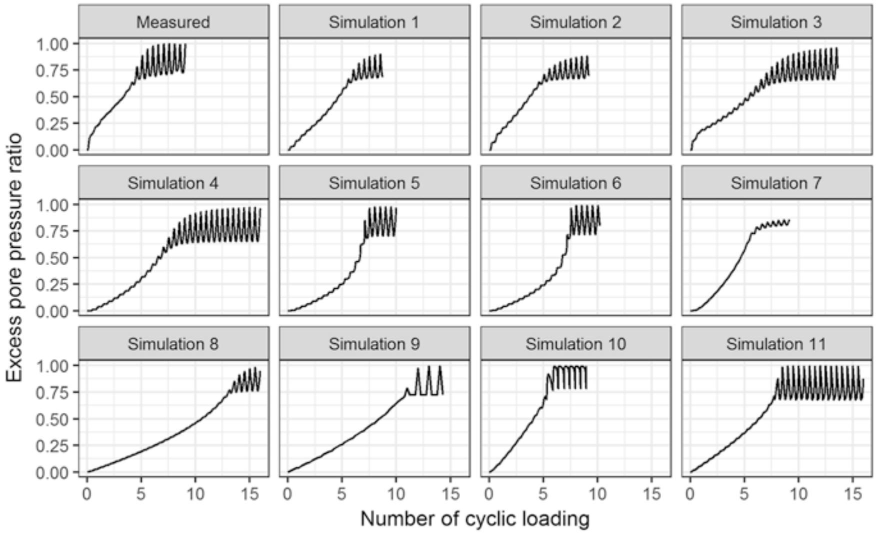

(a)

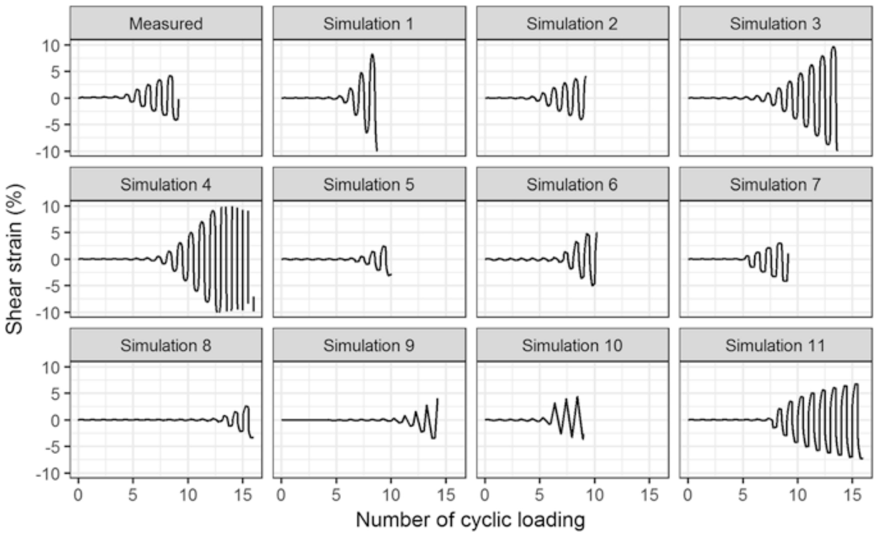

(b)

Fig. 2.5 Comparison of the numerical simulations of an undrained cyclic torsional shear test on Ottawa F-65 sand for Dr = 60%, CSR = 0.20. (**a**) Time history of excess pore pressure ratio, (**b**) Time history of shear strain, (**c**) Effective stress path, (**d**) Shear stress-shear strain relationship

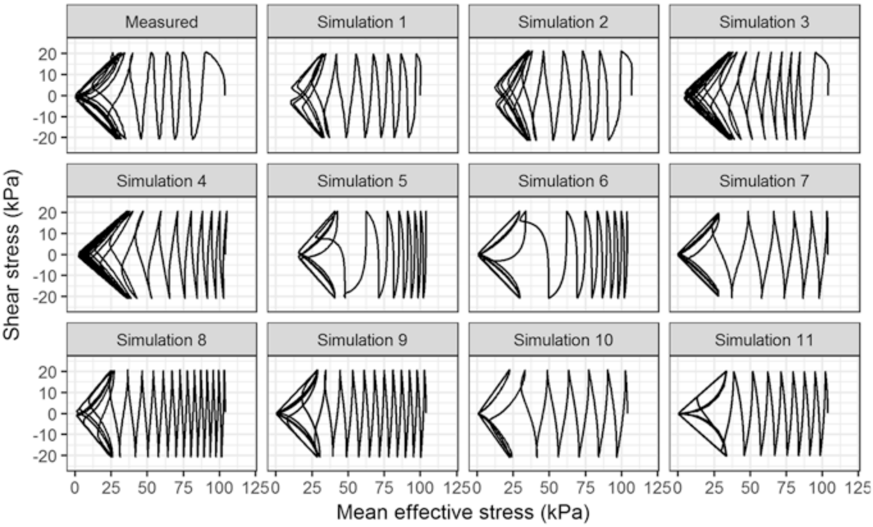

(c)

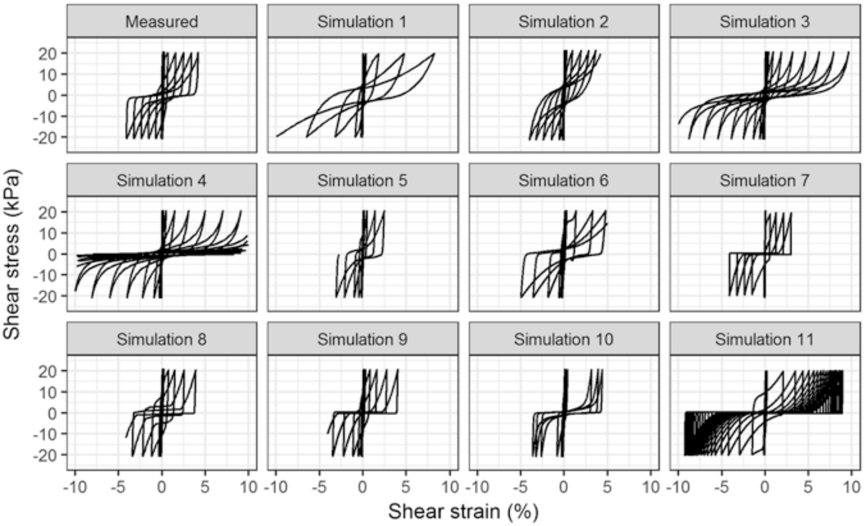

(d)

Fig. 2.5 (continued)

3. Simulations 5 and 6: Since the analysis platforms are different but the constitutive model is the same, the overall response tendency is very similar. The time history of the simulated excess pore water pressure shows that the pressure tends to rise rapidly at a certain stage, while it is relatively slow in the early stage of loading. This trend can also be seen in the simulated effective stress path.
4. Simulations 7 and 8: Although the constitutive model and the analysis platform are the same, the time history of the simulated excess pore water pressure, the effective stress path, and the associated strain development seem to be slightly

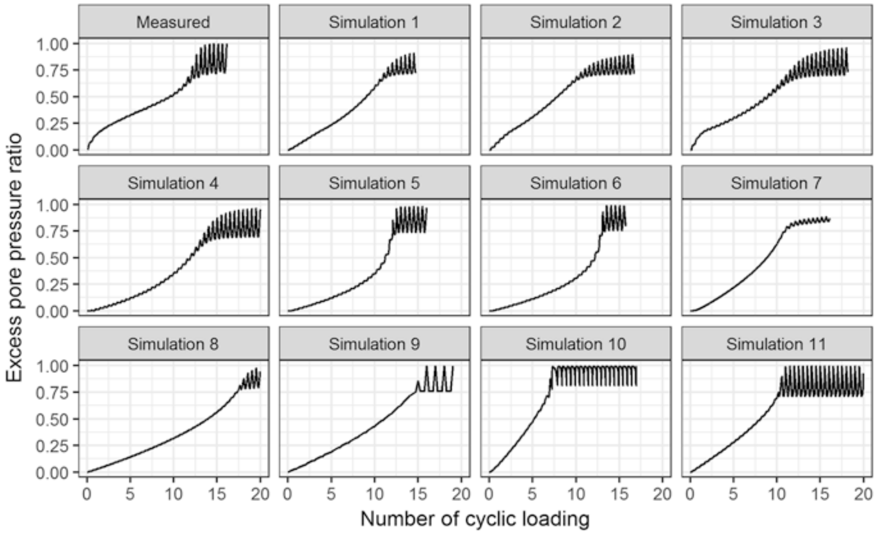

(a)

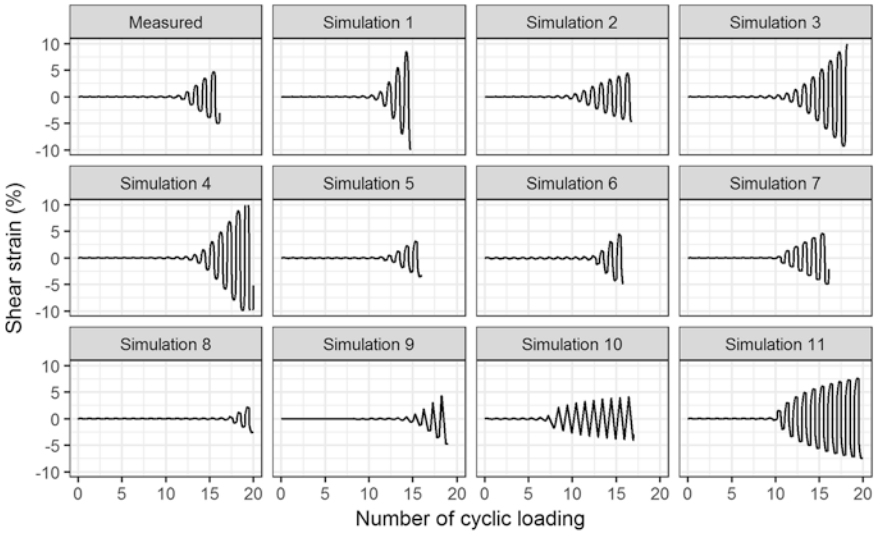

(b)

Fig. 2.6 Comparison of the numerical simulations of an undrained cyclic torsional shear test on Ottawa F-65 sand for Dr = 60%, CSR = 0.18. (**a**) Time history of excess pore pressure ratio, (**b**) Time history of shear strain, (**c**) Effective stress path, (**d**) Shear stress-shear strain relationship

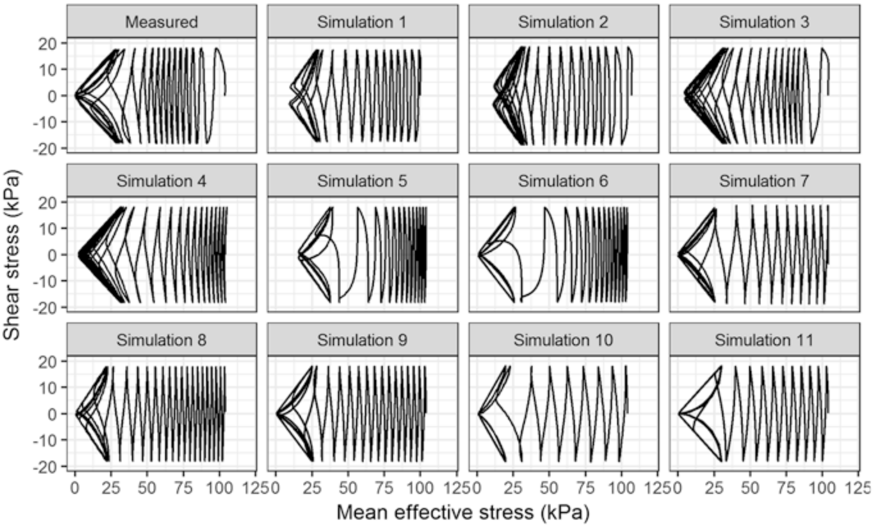

(c)

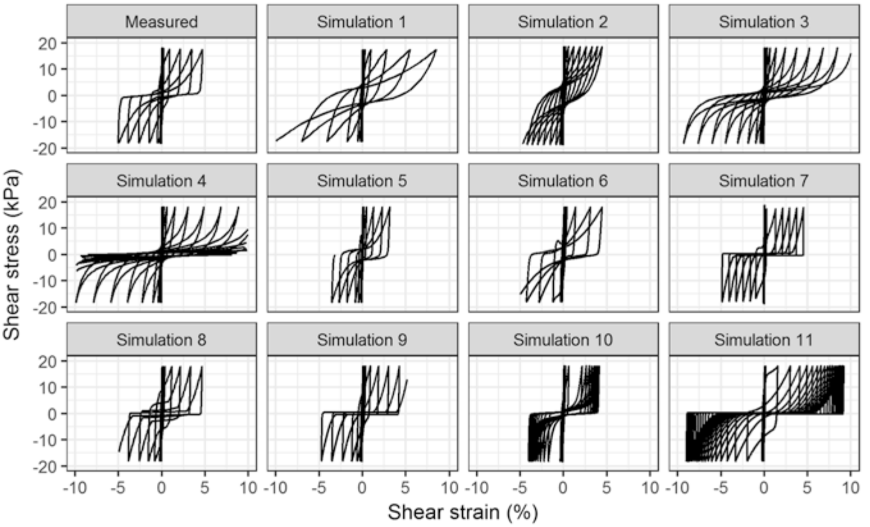

(d)

Fig. 2.6 (continued)

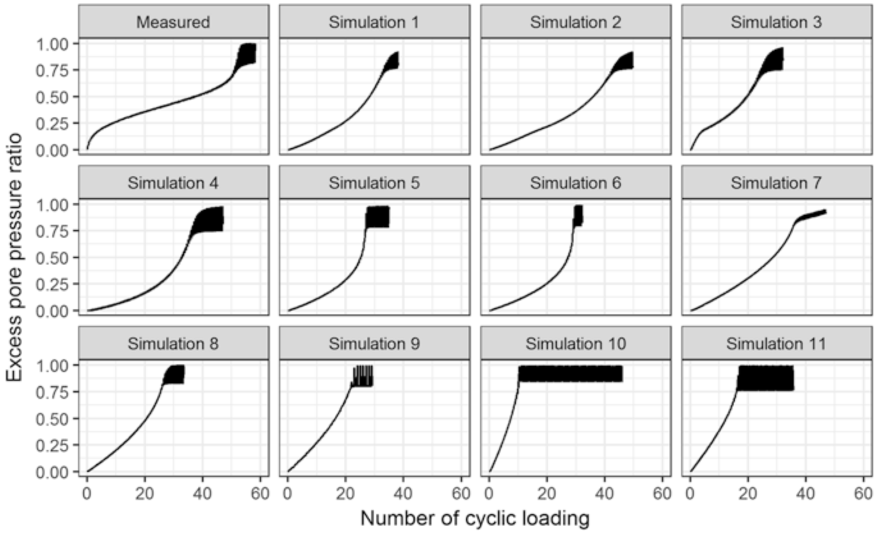

(a)

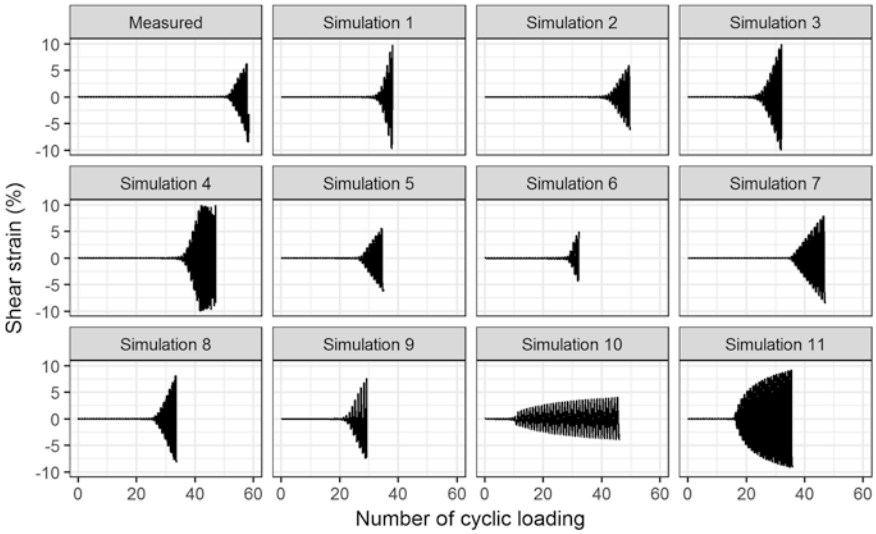

(b)

Fig. 2.7 Comparison of the numerical simulations of an undrained cyclic torsional shear test on Ottawa F-65 sand for Dr = 60%, CSR = 0.15. (**a**) Time history of excess pore pressure ratio, (**b**) Time history of shear strain, (**c**) Effective stress path, (**d**) Shear stress-shear strain relationship

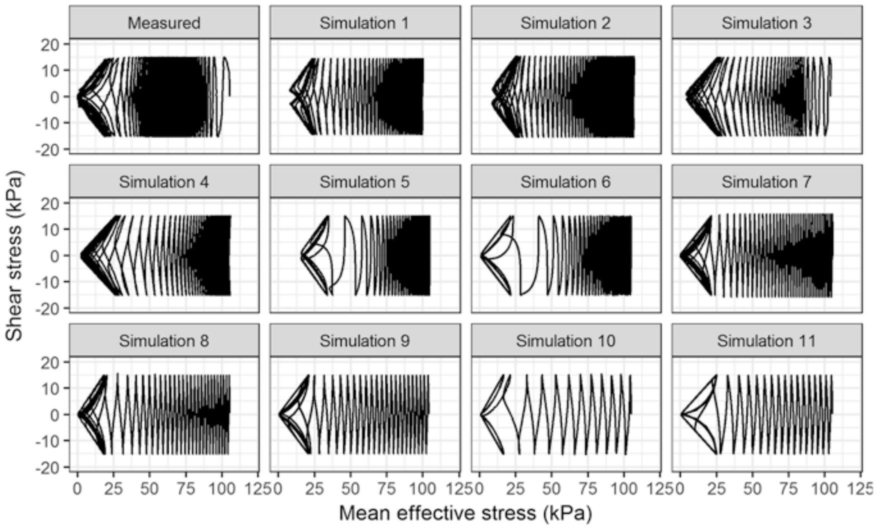

(c)

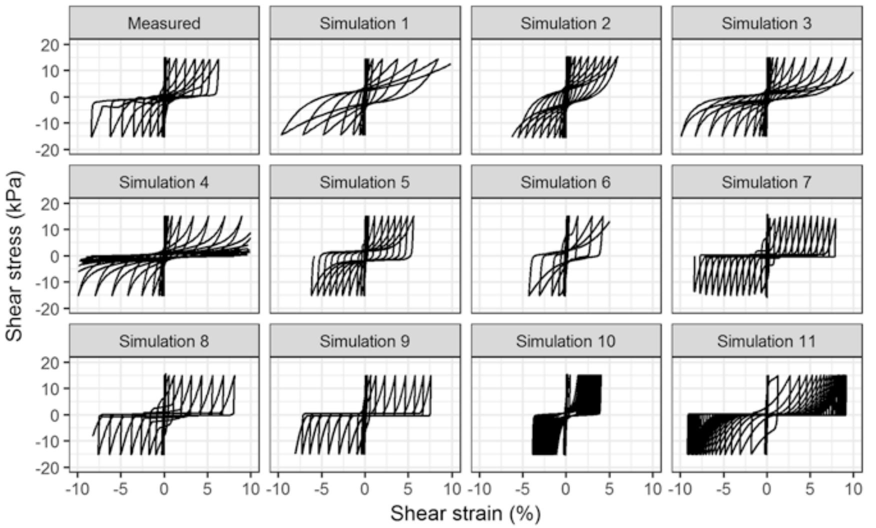

(d)

Fig. 2.7 (continued)

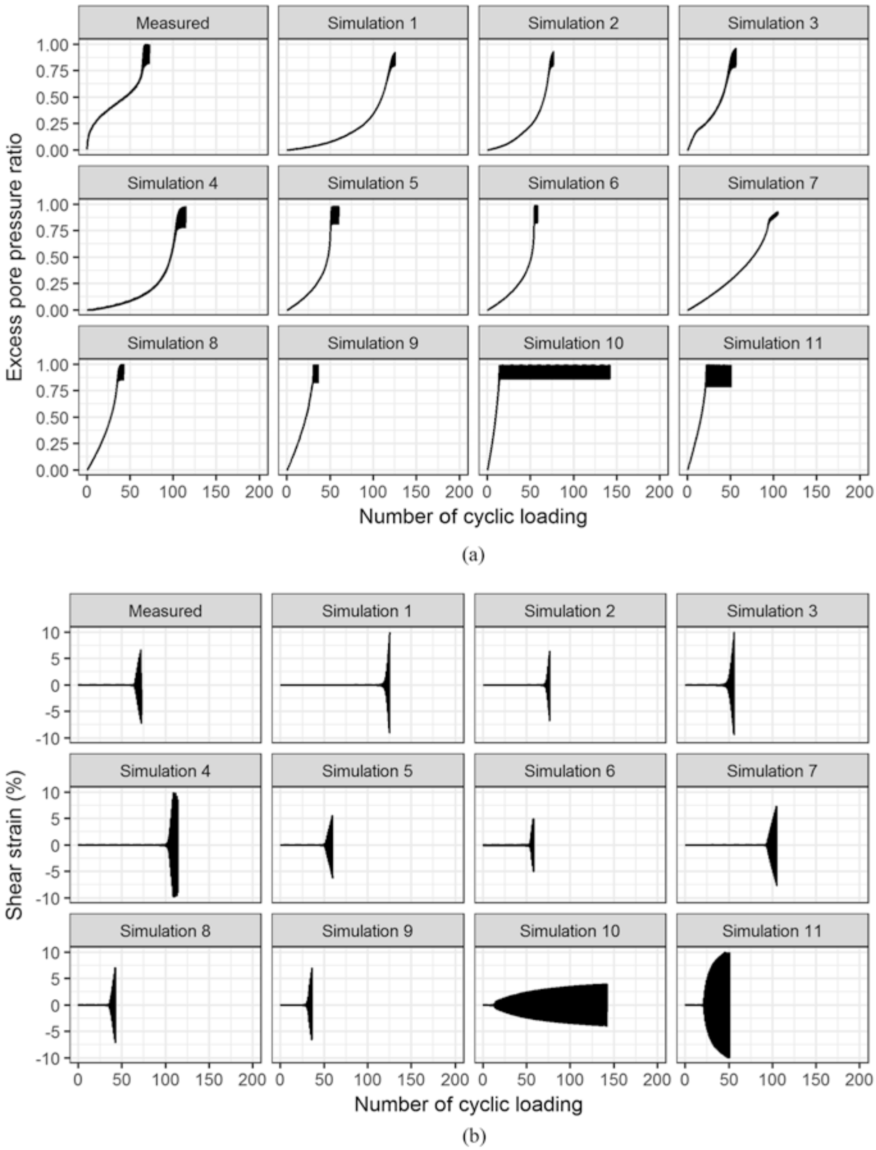

Fig. 2.8 Comparison of the numerical simulations of an undrained cyclic torsional shear test on Ottawa F-65 sand for Dr = 60%, CSR = 0.13. (**a**) Time history of excess pore pressure ratio, (**b**) Time history of shear strain, (**c**) Effective stress path, (**d**) Shear stress-shear strain relationship

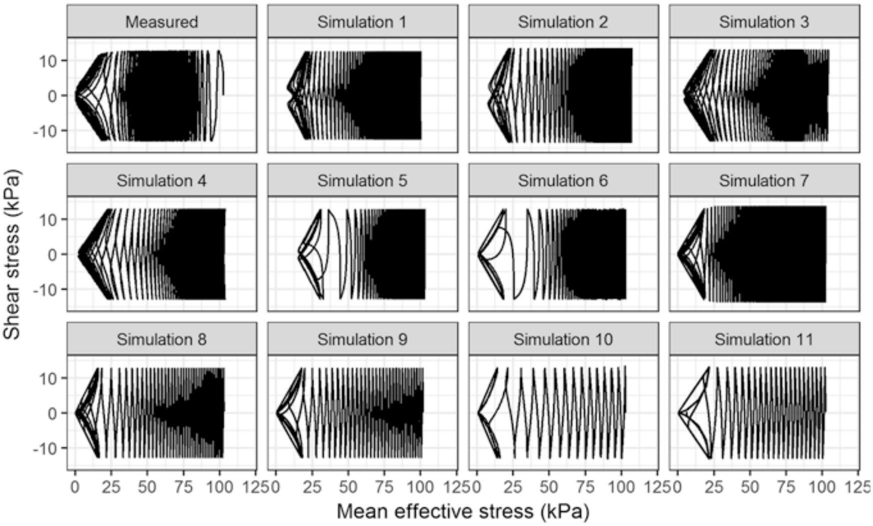

(c)

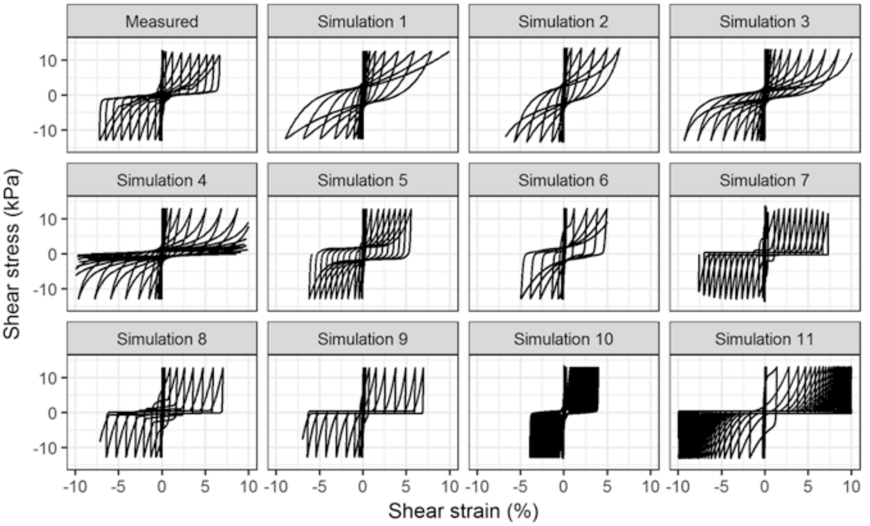

(d)

Fig. 2.8 (continued)

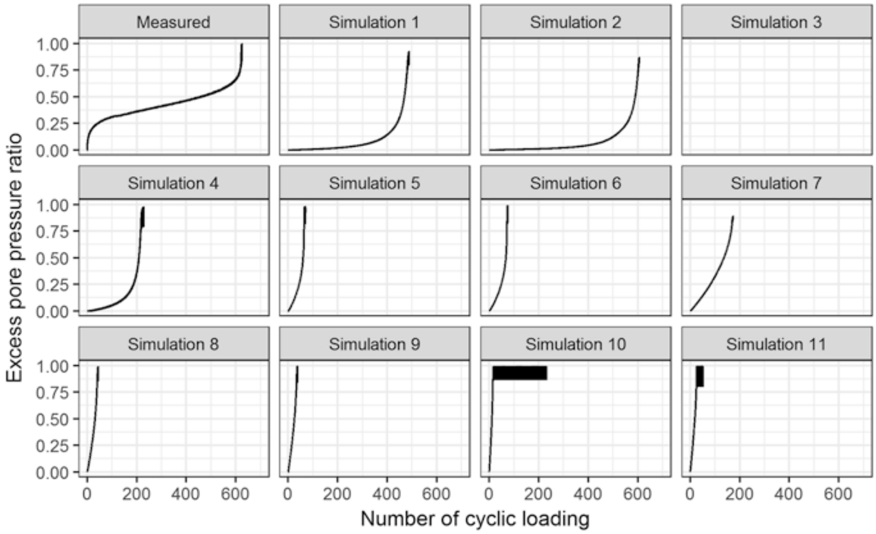

(a)

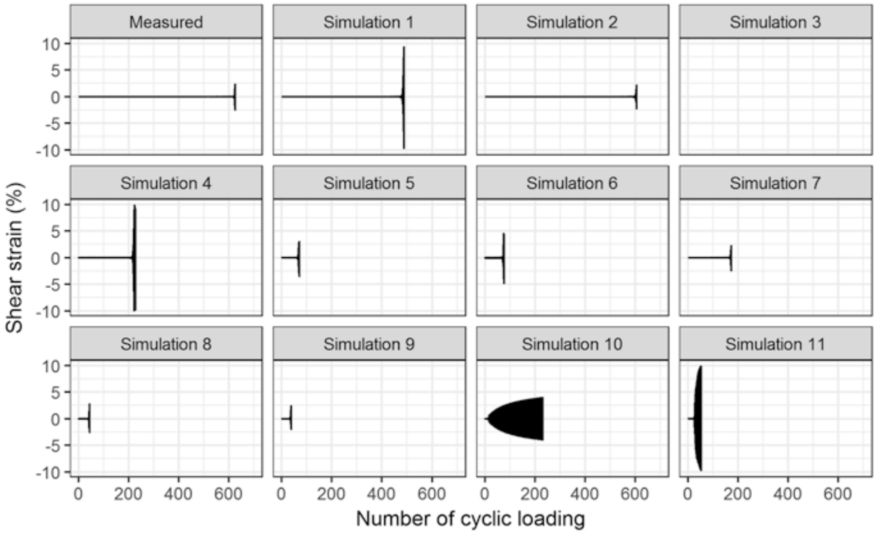

(b)

Fig. 2.9 Comparison of the numerical simulations of an undrained cyclic torsional shear test on Ottawa F-65 sand for Dr = 60%, CSR = 0.12. (**a**) Time history of excess pore pressure ratio, (**b**) Time history of shear strain, (**c**) Effective stress path, (**d**) Shear stress-shear strain relationship

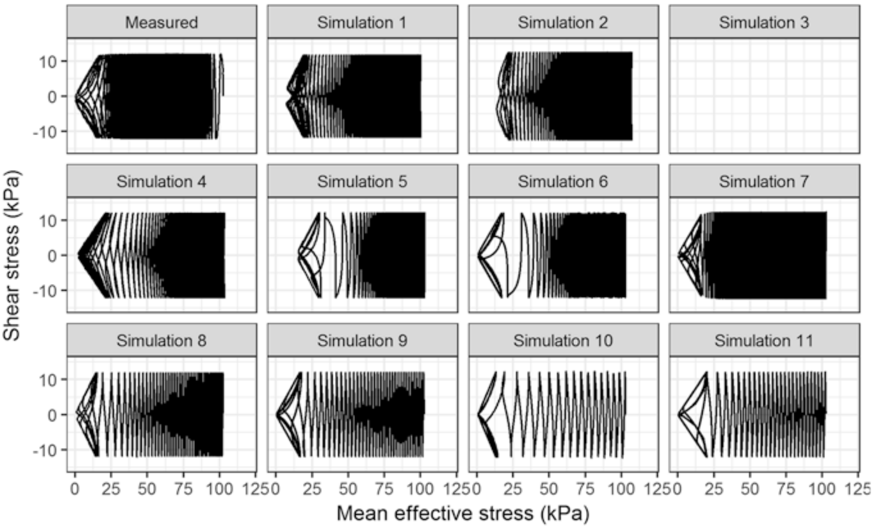

(c)

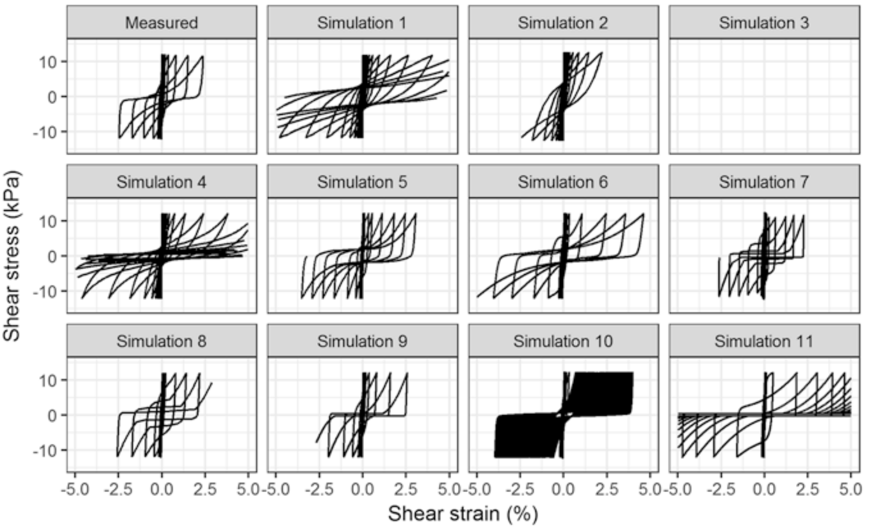

(d)

Fig. 2.9 (continued)

different. This is probably due to the difference in the values of the model parameters used.

5. Simulation 10: When the excess pore pressure ratio increases to 0.8–0.9, large shear strains are generated, which is common to other simulations. However, after that, the strain tends to extend relatively slowly; the strain development is almost linear.
6. Simulation 11: As in the other simulations, the shear strain begins to develop when the excess pore pressure ratio exceeds 0.8–0.9. However, the development is not linear and tends to converge gradually; the brittle behavior, in which the strain increases rapidly, is suppressed compared to the other simulations.

2.4 Liquefaction Resistance Curves

The simulated liquefaction resistance curves for γ_{DA} = 7.5% (i.e., the number of cycles required to reach a 7.5% double amplitude shear strain) are compared with the laboratory test results in Figs. 2.10a, b for Dr = 50% and 60%, respectively. The following trends are observed from the curves:

1. The majority of the constitutive models are capable of reasonably capturing the overall trends of the measured liquefaction resistance curves both for Dr = 50% and 60%; in particular, the liquefaction strength is accurately simulated for a cyclic stress ratio (CSR) of 0.149 and 0.174 for Dr = 50% and 60%, respectively.
2. Simulations 1–4: Since the constitutive model and the analysis platform are the same, the simulations show similar liquefaction resistance curves, although there are slight differences due to differences in the model parameters used. They can accurately simulate the experimental results even for low CSRs (i.e., a large number of cycles).
3. Simulations 5 and 6: Since the analysis platforms are different but the constitutive model is the same, the simulated liquefaction resistance curves are quite similar. The simulations are capable of reasonably simulating the experimental results, particularly in a relatively large CSR range.
4. Simulations 7 and 8: Although the constitutive model and the analysis platform are the same, the simulated liquefaction resistance curves look different; Simulation 8 shows steeper curves than the experimental curves, although both Simulations 7 and 8 can simulate the measured liquefaction strength for 20 cycles. The difference is probably due to the difference in the values of the model parameters used.
5. Simulation 10: The experimental curves are reasonably simulated over a wide range of CSRs, as in Simulations 1–4.
6. Simulations 9 and 11: The simulations show steeper curves than the experimental curves, although they can simulate the measured liquefaction strength for 10–20 cycles. It is unclear whether this is due to the characteristic of the constitutive models or the model parameters used.

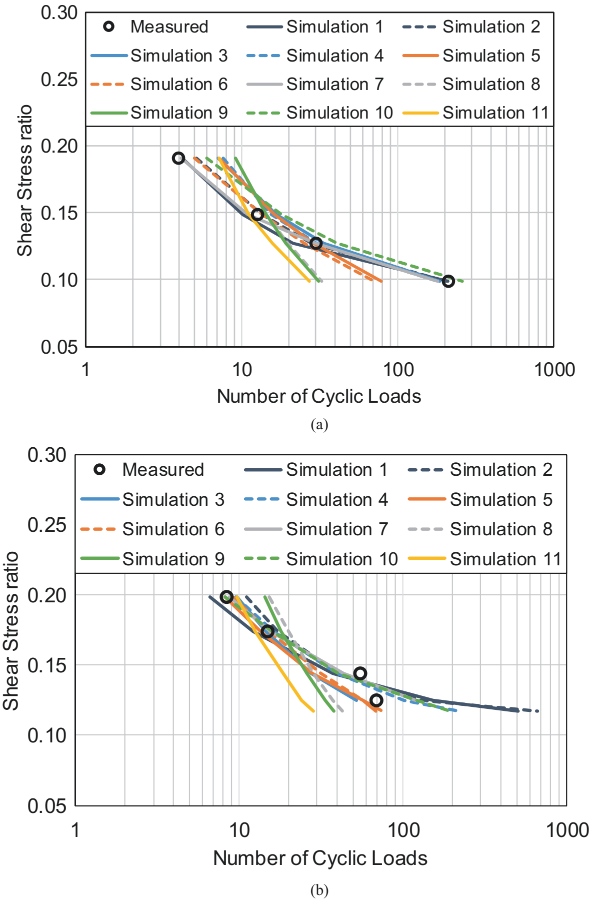

Fig. 2.10 Comparison of the simulated liquefaction strength curves by different numerical simulation teams with the experimental results reported by Ueda et al. (2018) and Vargas et al. (2020, 2023). (**a**) Dr = 50%, (**b**) Dr = 60%

2.5 Conclusions

This chapter presented a summary of the calibration exercises (i.e., element test simulations) submitted by nine numerical simulation teams that participated in the LEAP-ASIA-2019 prediction campaign. The objective of this element test simulation exercise was to assess the performance of the constitutive models used by the simulation teams for simulating the experimental results of a series of undrained stress-controlled cyclic torsional shear tests on Ottawa F-65 sand for two different relative densities (Dr = 50% and 60%). These simulations demonstrate that majority of the constitutive models are capable of reasonably capturing the measured liquefaction strength curves as well as the overall trends of the stress paths and stress-strain responses both for Dr = 50% and 60%. However, it appeared to be still left for future work to evaluate the validity of constitutive models in consideration of the variations in the laboratory test and/or numerical simulation results.

Acknowledgments The experimental work and numerical simulations on LEAP-ASIA-2019 were supported by different funds depending mainly on the location of the work. The work by the Japan PIs (Tobita, Ichii, Okamura, Takemura, and Ueda) was supported by JSPS KAKENHI grant number JP17H00846.

References

Bastidas, A. M. P. (2016). *Ottawa F-65 sand characterization*. Ph.D. Dissertation, University of California, Davis.

Bastidas, A. M. P., Boulanger, R. W., Carey, T., & DeJong, J. (2017). Ottawa F-65 sand data from Ana Maria Parra Bastidas, https://datacenterhub.org/resources/ottawa_f_65

El Ghoraiby, M. A., & Manzari, M. (2018). LEAP-2018 - stress-strain response of Ottawa F65 sand in cyclic simple shear, DesignSafe-CI [publisher], Dataset. https://doi.org/10.17603/DS2HX3H

El Ghoraiby, M. A., Park, H., & Manzari, M. T. (2019). Physical and mechanical properties of Ottawa F65 sand. In *Model tests and numerical simulations of liquefaction and lateral spreading: LEAP-UCD-2017*. Springer.

Elbadawy, M. A., & Zhou, Y. G. (2023). Class-C simulations of LEAP-ASIA-2019 via OpenSees platform by using a pressure dependent multi yield-surface model. In *Model tests and numerical simulations of liquefaction and lateral spreading: LEAP-ASIA-2019*. Springer.

Fasano, G., Chiaradonna, A., & Bilotta, E. (2023). LEAP-ASIA-2019 centrifuge test simulation at UNINA. In *Model tests and numerical simulations of liquefaction and lateral spreading: LEAP-ASIA-2019*. Springer.

Hyodo, J., & Ichii, K. (2023). LEAP-ASIA-2019 type-B simulations through FLIP at Kyoto University. In *Model tests and numerical simulations of liquefaction and lateral spreading: LEAP-ASIA-2019*. Springer.

Qiu, Z., & Elgamal, A. (2023). LEAP-ASIA-2019 centrifuge test simulations of liquefiable sloping ground. In *Model tests and numerical simulations of liquefaction and lateral spreading: LEAP-ASIA-2019*. Springer.

Reyes, A., Barrero, A. R., & Taiebat, M. (2023). Type-C simulations of centrifuge tests from LEAP-ASIA-2019 using SANISAND-sf. In *Model tests and numerical simulations of liquefaction and lateral spreading: LEAP-ASIA-2019*. Springer.

Tanaka, Y., Sahare, A., Ueda, K., Yuyama, W., & Iai, S. (2023). LEAP-ASIA-2019 numerical simulations using a strain space multiple mechanism model for a liquefiable sloping ground. In *Model tests and numerical simulations of liquefaction and lateral spreading: LEAP-ASIA-2019*. Springer.

Ueda, K., Vargas, R. R., & Uemura, K. (2018). LEAP-Asia-2018: Stress-strain response of Ottawa sand in cyclic torsional shear tests, DesignSafe-CI [publisher], Dataset. https://doi.org/10.17603/DS2D40H

Vargas, R. R., Ueda, K., & Uemura, K. (2020). Influence of the relative density and K0 effects in the cyclic response of Ottawa F-65 sand - cyclic torsional hollow-cylinder shear tests for LEAP-ASIA-2019. *Soil Dynamics and Earthquake Engineering, 133*, 106111.

Vargas, R. R., Ueda, K., & Uemura, K. (2023). Dynamic torsional shear tests of Ottawa F-65 sand for LEAP-ASIA-2019. In *Model tests and numerical simulations of liquefaction and lateral spreading: LEAP-ASIA-2019*. Springer.

Vasko, A. (2015). *An investigation into the behavior of Ottawa sand through monotonic and cyclic shear tests*. Master's thesis, The George Washington University.

Vasko, A., El Ghoraiby, M. A., & Manzari, M. T. (2018). *Characterization of Ottawa sand*. DesignSafe. https://doi.org/10.17603/DS2TH7Q

Wang, R., Zhu, T., Zhou, C., & Zhang, J. M. (2023). LEAP-ASIA-2019 simulations at Tsinghua University. In *Model tests and numerical simulations of liquefaction and lateral spreading: LEAP-ASIA-2019*. Springer.